



# Ferromagnetic exchange coupling in the linear, chloride-bridged cluster (cyclam)Co<sup>II</sup>[(μ-Cl)U<sup>IV</sup>(Me<sub>2</sub>Pz)<sub>4</sub>]<sub>2</sub>

Jeffrey D. Rinehart, Bart M. Bartlett, Stosh A. Kozimor, Jeffrey R. Long\*

Department of Chemistry, University of California, Berkeley, CA 94720-1460, United States

## ARTICLE INFO

### Article history:

Received 1 February 2008

Accepted 4 March 2008

Available online 10 March 2008

This work is dedicated to Prof. Dante Gatteschi

### Keywords:

5f–3d

Actinides

Uranium(IV)

Magnetic susceptibility

Exchange coupling

Clusters

## ABSTRACT

The trinuclear cluster (cyclam)Co[(μ-Cl)U(Me<sub>2</sub>Pz)<sub>4</sub>]<sub>2</sub> (cyclam = 1,4,8,11-tetraazacyclotetradecane, Me<sub>2</sub>Pz<sup>-</sup> = 3,5-dimethylpyrazolate) is synthesized through cleavage of the homoleptic dimer [U(Me<sub>2</sub>Pz)<sub>4</sub>]<sub>2</sub> by (cyclam)CoCl<sub>2</sub>. A single crystal X-ray diffraction analysis reveals a linear chloride-bridged structure analogous to that previously reported for (cyclam)M[(μ-Cl)U(Me<sub>2</sub>Pz)<sub>4</sub>]<sub>2</sub> (M = Ni, Cu, Zn). The magnetic exchange coupling of the CoU<sub>2</sub> cluster was probed by analyzing the temperature dependence of its magnetic susceptibility. Comparison of  $\chi_M T$  versus  $T$  between the CoU<sub>2</sub> species and the diamagnetic ZnU<sub>2</sub> cluster demonstrates the presence of ferromagnetic coupling between the Co<sup>II</sup> and U<sup>IV</sup> centers. We present methods for estimating upper and lower bounds for the exchange interaction energy in such systems and find that for CoU<sub>2</sub>, the exchange constant,  $J$ , lies in the range 15–48 cm<sup>-1</sup>. Application of these methods to the previously reported NiU<sub>2</sub> cluster suggests somewhat weaker ferromagnetic exchange, with  $J$  lying in the range 2.8–19 cm<sup>-1</sup>. AC magnetic susceptibility experiments were not indicative of single-molecule magnet behavior for the CoU<sub>2</sub> cluster, although qualitative interpretation of the low-temperature magnetization data suggests the presence of significant zero-field splitting in the ground state.

© 2008 Elsevier B.V. All rights reserved.

## 1. Introduction

Discrete molecules exhibiting slow magnetic relaxation as the consequence of a high-spin ground state with significant axial anisotropy are collectively known as single-molecule magnets. Initially, single-molecule magnets garnered much attention due to their potential application in information storage and quantum computing [1]. However, interest in such systems is tempered by the low blocking temperatures and small observed spin reversal barriers that give rise to facile thermal randomization and tunneling effects. Efforts to increase the spin reversal barrier have focused on both increasing the total spin of the molecule,  $S$ , and increasing the magnitude of the axial zero-field splitting parameter,  $D$ . These factors relate to the energy barrier through the equation  $U = S^2|D|$  (for integer values of  $S$ ). Given the second-power dependence on  $S$ , many studies have focused on synthesizing molecules that maximize total spin through coupling of large spin metal centers via superexchange. However, maximizing the axial anisotropy presents a greater challenge, as it is often more difficult to predict the sign and magnitude of  $D$  for the overall molecular cluster.

The f-elements should be particularly well-suited for maximizing  $D$  due to increased coupling between spin and orbital angular

momenta [2], and recent efforts have exploited the large single-ion anisotropy of lanthanides to generate spin reversal barriers [3]. Nevertheless, the contracted 4f orbitals preclude strong coupling between multiple metal centers [4]. Actinides offer an intriguing alternative, in that the single-ion anisotropy should remain large, and the magnetic exchange coupling should be strengthened by the increased radial extension of the 5f orbitals [5]. Despite these advantages, quantitative studies of magnetic coupling in actinide-containing systems remain relatively rare [6] due to the innate complications of the large spin–orbit coupling present in actinide elements. Herein, we present the synthesis of a new chloride-bridged 5f–3d trinuclear cluster, (cyclam)-Co[(μ-Cl)U(Me<sub>2</sub>Pz)<sub>4</sub>]<sub>2</sub> (cyclam = 1,4,8,11-tetraazacyclotetradecane, Me<sub>2</sub>Pz<sup>-</sup> = ce:hsp sp="0.25"/>3,5-dimethylpyrazolate), and propose a magnetic model for estimating upper and lower bounds for its exchange parameter,  $J$ .

## 2. Synthesis and characterization

### 2.1. General considerations

The syntheses and manipulations of the extremely air and moisture sensitive compounds described below were conducted under nitrogen with rigorous exclusion of air and water by Schlenk and glovebox techniques. Dichloromethane was saturated with N<sub>2</sub>, passed through an activated alumina column, degassed by three

\* Corresponding author.

E-mail address: jrlong@berkeley.edu (J.R. Long).

freeze–pump–thaw cycles, and stored under N<sub>2</sub> over 3-Å molecular sieves. Benzene-*d*<sub>6</sub> (Cambridge Isotope Laboratories) was distilled over sodium–potassium alloy with benzophenone and degassed by three freeze–pump–thaw cycles. Methanol was distilled over magnesium and iodine and saturated with N<sub>2</sub>. The compounds [U(Me<sub>2</sub>Pz)<sub>4</sub>]<sub>2</sub> and (cyclam)M[(μ-Cl)U(Me<sub>2</sub>Pz)<sub>4</sub>]<sub>2</sub> (M = Zn, Ni) were synthesized as previously described [6g]. NMR spectroscopy experiments were conducted using a Bruker 400 MHz spectrometer. UV–Vis absorption spectra were measured in 1-cm path length quartz cuvettes equipped with Teflon sealable stopcocks and recorded on a Cary 5000 spectrophotometer. Elemental analyses were performed by the analytical laboratories at the University of California, Berkeley.

## 2.2. Magnetic measurements

Powder microcrystalline magnetic samples were prepared in a frozen eicosane matrix and sealed in quartz tubes under vacuum. Magnetic susceptibility measurements were collected using a Quantum Design MPMS2 SQUID magnetometer. DC susceptibility data measurements were performed at temperatures ranging from 5 to 300 K, using applied fields of 0.1, 0.5, and 1 T. Magnetization measurements were performed at temperatures ranging from 1.8 to 10 K under an applied magnetic field varying from 1 to 7 T at 1 T intervals.

All magnetic data were corrected for the diamagnetic contributions from the quartz sample holder and eicosane, as well as for the core diamagnetism of each sample. Core diamagnetism was estimated using Pascal's constants to give  $\chi_D = -2.13 \times 10^{-4}$ ,  $-7.75 \times 10^{-4}$ , and  $-7.78 \times 10^{-4}$  emu/mol for (cyclam)CoCl<sub>2</sub>, (cyclam)Co[(μ-Cl)U(Me<sub>2</sub>Pz)<sub>4</sub>]<sub>2</sub>, and (cyclam)Zn[(μ-Cl)U(Me<sub>2</sub>Pz)<sub>4</sub>]<sub>2</sub>, respectively.

## 2.3. X-ray crystallography

Crystallographic data for (cyclam)Co[(μ-Cl)U(Me<sub>2</sub>Pz)<sub>4</sub>]<sub>2</sub> · 4CH<sub>2</sub>Cl<sub>2</sub> are presented in Table 1. A crystal was mounted on a Kapton loop and transferred to a Bruker APEX diffractometer and cooled in a nitrogen stream. The SMART [7] program package was used to determine the unit cell parameters and for data collection (30 s/frame scan time for a hemisphere of diffraction data). Data integration was performed by SAINT [8]

**Table 1**  
Crystallographic data for (cyclam)Co[(μ-Cl)U(Me<sub>2</sub>Pz)<sub>4</sub>]<sub>2</sub> · 4CH<sub>2</sub>Cl<sub>2</sub>

Empirical formula	U <sub>2</sub> CoCl <sub>10</sub> N <sub>20</sub> C <sub>54</sub> H <sub>88</sub>
Formula weight	1906.93
Temperature (K)	166(2)
Wavelength (Å)	0.71073
Crystal system	triclinic
Space group	P $\bar{1}$
<i>Unit cell dimensions</i>	
<i>a</i> (Å)	11.440(3)
<i>b</i> (Å)	12.178(4)
<i>c</i> (Å)	14.903(4)
$\alpha$ (°)	72.408(5)
$\beta$ (°)	77.100(5)
$\gamma$ (°)	73.871(4)
Volume (Å <sup>3</sup> )	1879.1(10)
<i>Z</i>	1
<i>D</i> <sub>calc</sub> (Mg/m <sup>3</sup> )	1.685
Absorption coefficient (mm <sup>-1</sup> )	4.920
Crystal size (mm)	0.13 × 0.12 × 0.03
$\theta$ Range for data collection (°)	1.45–23.32
Data/restraints/parameters	5386/0/394
Final <i>R</i> indices [ <i>I</i> > 2σ( <i>I</i> )]	<i>R</i> <sub>1</sub> = 0.0450, <i>wR</i> <sub>2</sub> = 0.0875
<i>R</i> indices (all data)	<i>R</i> <sub>1</sub> = 0.0677, <i>wR</i> <sub>2</sub> = 0.0937
Largest difference in peak and hole (e <sup>-</sup> Å <sup>-3</sup> )	1.242 and –1.000

and the absorption correction provided by SADABS [9]. Subsequent calculations were carried out using the SHELXTL program [10]. The structure was solved by direct methods and refined on *F*<sup>2</sup> by full-matrix least-squares techniques. The analytical scattering factors for neutral atoms [11] were used throughout the analysis. Hydrogen atoms were included using a riding model.

## 2.4. (cyclam)CoCl<sub>2</sub>

A solution of CoCl<sub>2</sub> (50 mg, 0.39 mmol) in 3 mL of methanol was added dropwise to a solution of cyclam (77 mg, 0.39 mmol) in 3 mL of methanol to form a pink solution. After stirring for 3 h, the solution was cooled to –25 °C for 24 h. The resulting pink needle-like crystals were collected by filtration and washed with methanol (3 × 5 mL). The crystals were then dried under reduced pressure at 50 °C for 3 h to give 81 mg (64%) product. *Anal. Calc.* for C<sub>10</sub>H<sub>24</sub>Cl<sub>2</sub>CoN<sub>4</sub>: C, 36.38; H, 7.33; N, 16.97. Found: C, 36.34; H, 7.51; N, 16.54%.

## 2.5. (cyclam)Co[(μ-Cl)U(Me<sub>2</sub>Pz)<sub>4</sub>]<sub>2</sub>

A solution of [U(Me<sub>2</sub>Pz)<sub>4</sub>]<sub>2</sub> (200 mg, 0.16 mmol) in dichloromethane (8 mL) was added dropwise to a solution of (cyclam)CoCl<sub>2</sub> (54 mg, 0.16 mmol) in dichloromethane (8 mL) to form a green solution. After stirring for 12 h, the solution was filtered through Celite, concentrated to approximately 5 mL under reduced pressure, and cooled to –25 °C for 24 h. The resulting green block-shaped crystals were isolated by decanting the green supernatant solution. The crystals were dried under reduced pressure to give 110 mg (43%) of product. <sup>1</sup>H NMR (CH<sub>2</sub>Cl<sub>2</sub> referenced to a C<sub>6</sub>D<sub>6</sub> internal standard, 292 K):  $\delta$  –36 ( $\Delta\nu_{1/2}$  = 3200 Hz), –15 ( $\Delta\nu_{1/2}$  = 2000 Hz) 6 ( $\Delta\nu_{1/2}$  = 280 Hz), 15 ( $\Delta\nu_{1/2}$  = 800 Hz) ppm. Accurate integrations and peak assignments were not possible due to the paramagnetic nature of the complex. Absorption spectrum (CH<sub>2</sub>Cl<sub>2</sub>):  $\lambda_{\max}$  ( $\epsilon_M$ ) 234 (5965), 328 (sh, 4030), 479 (66), 506 (45), 562 (19), 626 (32) 678 (67), 870 (17), 924 (18) nm. *Anal. Calc.* for C<sub>50</sub>H<sub>80</sub>Cl<sub>2</sub>CoN<sub>20</sub>U<sub>2</sub>: C, 38.31; H, 5.16; N, 17.88. Found: C, 38.43; H, 5.34; N, 17.92%.

## 3. Results and discussion

Cleavage of the [U(Me<sub>2</sub>Pz)<sub>4</sub>]<sub>2</sub> dimer by (cyclam)CoCl<sub>2</sub> affords the trinuclear cluster (cyclam)Co[(μ-Cl)U(Me<sub>2</sub>Pz)<sub>4</sub>]<sub>2</sub> in moderate yield. The structure (see Fig. 1) is centrosymmetric with an inversion center located on the central cobalt atom; four CH<sub>2</sub>Cl<sub>2</sub> molecules also occupy the unit cell. The metric parameters of the cluster are listed in Table 2 together with those of the previously synthesized analogues (cyclam)M[(μ-Cl)U(Me<sub>2</sub>Pz)<sub>4</sub>]<sub>2</sub> (M = Ni, Cu,

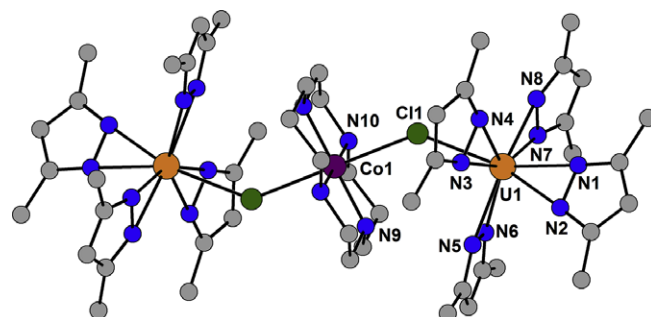


**Fig. 1.** Structure of the linear cluster (cyclam)Co[(μ-Cl)U(Me<sub>2</sub>Pz)<sub>4</sub>]<sub>2</sub>. Orange, purple, green, gray, and blue spheres represent U, Co, Cl, C, and N atoms, respectively; H atoms are omitted for clarity. The cluster resides on an inversion center within the crystal. Atom labels correspond to those referenced in Table 2.

**Table 2**

Selected interatomic distances (Å) and angles (°) observed for (cyclam)M[(μ-Cl)U(Me<sub>2</sub>Pz)<sub>4</sub>]<sub>2</sub> (MU<sub>2</sub>; M = Co, Ni, Cu, Zn)

	CoU <sub>2</sub>	NiU <sub>2</sub>	CuU <sub>2</sub>	ZnU <sub>2</sub>
U(1)–Cl(1)	2.800(2)	2.838(2)	2.785(2)	2.822(2)
M(1)–Cl(1)	2.668(2)	2.564(2)	2.774(2)	2.680(2)
U(1)–N(1)	2.393(7)	2.375(8)	2.396(6)	2.392(5)
U(1)–N(2)	2.389(7)	2.388(8)	2.390(6)	2.380(5)
U(1)–N(3)	2.385(7)	2.397(8)	2.392(6)	2.387(5)
U(1)–N(4)	2.377(7)	2.400(8)	2.385(5)	2.406(5)
U(1)–N(5)	2.413(7)	2.401(8)	2.415(6)	2.423(5)
U(1)–N(6)	2.433(7)	2.419(7)	2.427(6)	2.414(5)
U(1)–N(7)	2.388(7)	2.386(8)	2.390(6)	2.381(5)
U(1)–N(8)	2.427(11)	2.389(7)	2.407(6)	2.392(5)
M(1)–N(9)	1.962(7)	2.059(8)	2.017(6)	2.087(5)
M(1)–N(10)	1.983(6)	2.063(8)	2.022(5)	2.082(5)
U(1)–Cl(1)–M(1)	138.76(8)	139.47(9)	137.61(7)	138.31(6)

Zn) for comparison [6g]. Of particular note, the structure of the CoU<sub>2</sub> cluster is extremely similar to that of the ZnU<sub>2</sub> cluster, such that the latter can be used as a reasonable model in accounting for the U<sup>IV</sup> contributions to the magnetism of the former. The similarity between the 2.68(2) and 2.680(2) Å M–Cl (M = Co and Zn) distances in CoU<sub>2</sub> and ZnU<sub>2</sub>, respectively, is somewhat unexpected, since the observed Co–Cl distance is significantly longer than analogous bond lengths typically observed (2.282–2.522 Å) in species featuring Co<sup>II</sup> centers bridged to another transition metal through chloride [12]. We note in our previous study of NiU<sub>2</sub> and CuU<sub>2</sub>, that the Ni–Cl distance of 2.564(2) Å engenders ferromagnetic coupling between Ni<sup>II</sup> and U<sup>IV</sup>, but that the long Cu–Cl distance of 2.774(2) Å gives rise to a complex that shows no magnetic coupling. In CoU<sub>2</sub>, the Co–Cl distance is intermediary while the 1.973(14) Å average Co–N distance is similar to the analogous distances in the NiU<sub>2</sub> and CuU<sub>2</sub> complexes, cf. 2.061(3) and 2.020(4) Å, respectively. This suggests that magnetically, the system might be best described as containing a low-spin ( $S = 1/2$ ) Co<sup>II</sup> complex with the longer Co–Cl bond distances arising from a 1st order Jahn–Teller distortion [13]. This unpaired electron resides in d<sub>z<sup>2</sup></sub> and is therefore oriented directly along the superexchange pathway. This may provide sufficient better orbital overlap to open the possibility of magnetic coupling despite the unusually long Co–Cl bond distance. In contrast, for CuU<sub>2</sub>, the Jahn–Teller distortion results in an elongated Cu–Cl bond where the unpaired electron occupies d<sub>x<sup>2</sup>-y<sup>2</sup></sub>, orthogonal to the exchange pathway.

As an initial probe of the spin of Co<sup>II</sup> center in the cluster, we collected magnetic susceptibility data of the precursor complex (cyclam)CoCl<sub>2</sub>. Fig. 2 shows the resulting  $\chi_M T$  product of 0.41 emu K/mol, which is essentially invariant with temperature, indicative of an  $S = 1/2$  compound. The lack of variance in  $\chi_M T$  with temperature obviates the likelihood that spin–orbit coupling in high-spin Co<sup>II</sup> results in the observed  $S = 1/2$  behavior [14], since this normally only occurs through a gradual loss of spin from  $S = 3/2$  at room temperature to  $S = 1/2$  at low temperature (<40 K). This will greatly simplify the modeling of the magnetic data for the CoU<sub>2</sub> cluster by eliminating the need to account for Co<sup>II</sup> spin–orbit coupling.

The problems associated with interpreting f-element magnetic behavior arise from a confluence of factors. The predominant issue is the breakdown of the spin-only approximation arising from coupling of the orbital angular momentum to the spin angular momentum within the degenerate f-orbitals. In addition, actinide elements tend to display greater covalency in their bonding than lanthanide elements, such that spin loss resulting from the presence of ligand field effects cannot be ignored. The ligand field, albeit weak, removes the degeneracy of the f-orbitals and gives rise to some degree of spin pairing and must also be considered.

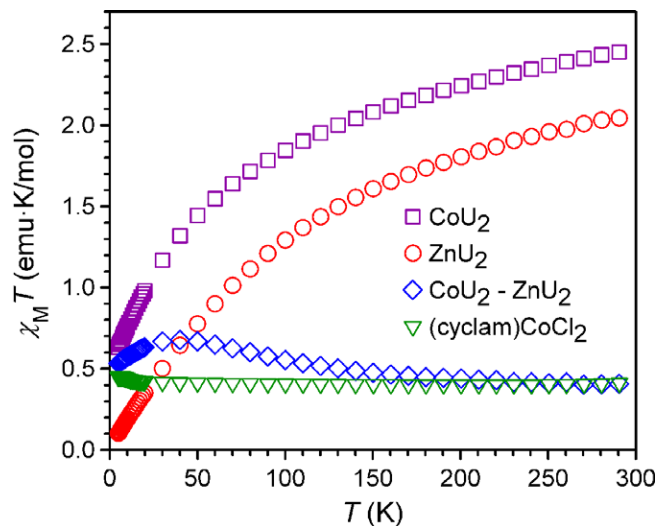


**Fig. 2.** Variable-temperature magnetic susceptibility data for the trinuclear cluster (cyclam)Co[(μ-Cl)U(Me<sub>2</sub>Pz)<sub>4</sub>]<sub>2</sub> (CoU<sub>2</sub>, purple squares) and its previously published analogue, (cyclam)Zn[(μ-Cl)U(Me<sub>2</sub>Pz)<sub>4</sub>]<sub>2</sub> (ZnU<sub>2</sub>, red circles). Blue diamonds correspond to a subtraction of the ZnU<sub>2</sub> data from the CoU<sub>2</sub> data. Magnetic data for the precursor complex (cyclam)CoCl<sub>2</sub> are depicted as green triangles.

The magnetic susceptibility data for the ZnU<sub>2</sub> cluster, illustrated in Fig. 2, demonstrates the decaying effect in  $\chi_M T$  with decreasing temperature resulting from the influence of a combination of these factors on the spin of the U<sup>IV</sup> centers. These deviations from spin-only behavior significantly hinder the observation of magnetic exchange coupling between an actinide metal and another metal. While it is not feasible to distinguish between spin–orbit coupling effects and ligand field effects solely through the magnetic properties, we can devise two models to correct for the observed spin loss. The first takes into account that at low temperatures, the strong spin–orbit coupling in U<sup>IV</sup> dominates the magnetism. As described in quantitative detail below, our strategy is to subtract out all contributions from U<sup>IV</sup>, leaving only the transition-metal spin and residual exchange coupling. In this way, we isolate the magnetism of the actinide from the transition metal, and fit the data by adding back an imposed spin-only value for U<sup>IV</sup>. In our second model, we treat the actinide and transition metal together by empirically factoring the data to account for both the effects of exchange coupling mediated through U–Cl covalency and spin–orbit coupling inherent to U<sup>IV</sup>. We consider that as the temperature drops, the observed moment of MU<sub>2</sub> complexes immediately drops, even for ZnU<sub>2</sub>, which should behave as a system containing isolated U<sup>IV</sup> spins. It is important to note that at room temperature, ZnU<sub>2</sub> does display spin-only behavior such that our reduction factor is physically meaningful. The factored data corrects for spin–orbit coupling and ligand field effects, such that any deviation from the spin-only value for any given cluster is due to exchange coupling of the magnetic ions that comprise the cluster. In this way, we estimate lower and upper bounds for the exchange energy between the spins on both uranium(IV) centers and the transition metal.

The temperature-dependent magnetic susceptibility data for CoU<sub>2</sub> and ZnU<sub>2</sub> display qualitatively similar trends and are dominated by a reduction in the effective spin of the 5f<sup>2</sup> configuration of U<sup>IV</sup> as the temperature decreases (see Fig. 2). We note that at room temperature, the  $\chi_M T$  values are near the expected spin-only values. At 300 K,  $\chi_M T = 2.06$  emu K/mol for the ZnU<sub>2</sub> cluster, as expected for two uncoupled U<sup>IV</sup> ions, and  $\chi_M T = 2.47$  emu K/mol for CoU<sub>2</sub>, corresponding well with the expectation for two uncoupled U<sup>IV</sup> ions and one low-spin Co<sup>II</sup> ion. However, as the temperature is

lowered, the two compounds display somewhat different behavior, in that the  $\chi_M T$  value decays less rapidly for CoU<sub>2</sub>. Since the structures are similar (see Table 2), differences in the ligand field about uranium(IV) alone cannot account for this variation in the decay of  $\chi_M T$ . Rather, this difference suggests the presence of magnetic exchange coupling between the Co<sup>II</sup> and U<sup>IV</sup> centers in the CoU<sub>2</sub> cluster.

In order to estimate the magnitude of the exchange energy, we can first attempt to extract the component of the magnetic susceptibility due to the Co<sup>II</sup> center from that of U<sup>IV</sup>, and subsequently reinstate an idealized spin-only U<sup>IV</sup> susceptibility. Subtraction of the ZnU<sub>2</sub> data from the CoU<sub>2</sub> data should yield  $\chi_M T$  for an isolated d<sup>7</sup> Co<sup>II</sup> ion together with any residual moment due to exchange coupling. The plot of this subtracted data, shown in blue in Fig. 2, is consistent with an isolated Co<sup>II</sup> center at high temperature, and corresponds to the observed  $\chi_M T$  value of 0.41 emu K/mol, independently measured for (cyclam)CoCl<sub>2</sub>. However, as the temperature drops,  $\chi_M T$  begins to rise, reaching a maximum of 0.68 emu K/mol at 40 K. This elevation of  $\chi_M T$  at low temperature is indicative of ferromagnetic exchange between the U<sup>IV</sup> and Co<sup>II</sup> metal centers. To estimate the strength of the exchange coupling, MAGFIT 3.1 [15] was employed to fit the subtracted magnetic susceptibility data above 70 K (where an inflection point occurs in the data) using a spin Hamiltonian of the form  $\hat{H} = -2J[\hat{S}_{\text{Co}} \cdot (\hat{S}_{\text{U}(1)} + \hat{S}_{\text{U}(2)})] + g\mu_B \mathbf{S} \cdot \mathbf{B}$ . In order to account for a spin-only ( $S = 1$ ) contribution from the two U<sup>IV</sup> centers to the total spin, a temperature-invariant contribution of 2.00 emu K/mol was added back into the data. Optimization of the fit parameters gave  $J = 15 \text{ cm}^{-1}$ ,  $g = 1.92$ , and  $\text{TIP} = 3.16 \times 10^{-4} \text{ emu/mol}$ . The adjusted data as well as the optimized fit for the CoU<sub>2</sub> cluster are shown in Fig. 3 (blue diamonds). Reoptimization of the data for the NiU<sub>2</sub> cluster from our previous work leads to a slight increase in  $J$  from  $2.3 \text{ cm}^{-1}$  to  $2.8 \text{ cm}^{-1}$ , with  $g = 1.96$  and  $\text{TIP} = 5.15 \times 10^{-4} \text{ emu/mol}$  (Fig. 3, red circles). We note that these  $J$  values represent only a lower bound on the exchange energy, because the foregoing treatment eliminates the effects of spin-orbital contributions and ligand field effects, but only subsequently accounts for the spin at the U<sup>IV</sup> centers by adding a constant contribution of 2.00 emu K/mol for the two U<sup>IV</sup> centers.

In an effort to provide an upper bound for the exchange energy, we propose a second model in which we assume that the reduction

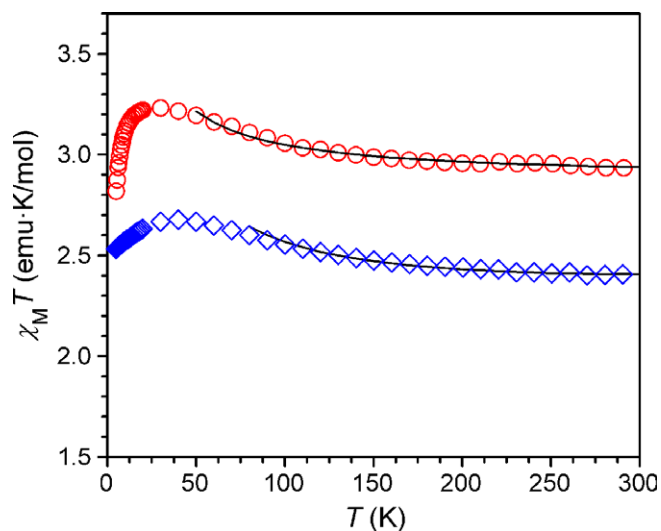


**Fig. 3.** Empirical  $\chi_M T$  data arising upon subtraction of the ZnU<sub>2</sub> cluster data from the CoU<sub>2</sub> (blue diamonds) and NiU<sub>2</sub> (red circles) cluster data. A calculated value of 2.00 emu K/mol has been added to represent a spin-only contribution from the U<sup>IV</sup> centers. Best calculated fits to the data are shown as black lines ( $J_{\text{min}}(\text{Co}) = 15 \text{ cm}^{-1}$ ,  $J_{\text{min}}(\text{Ni}) = 2.8 \text{ cm}^{-1}$ ); see text for details.

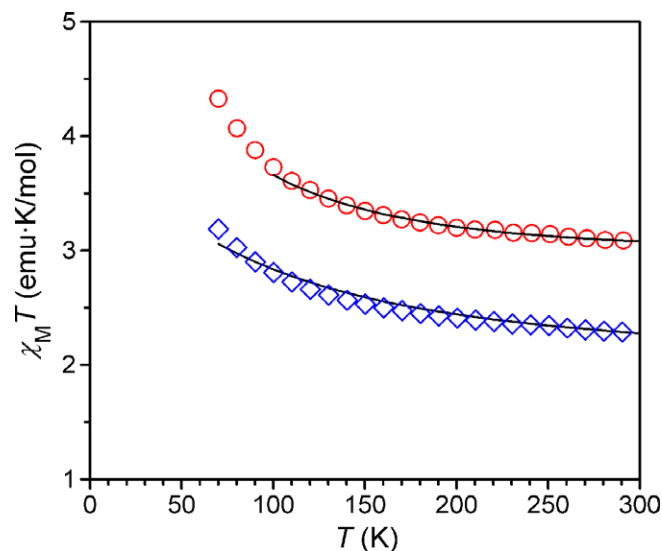


**Fig. 4.** Plots of  $\chi_M T$  data for the CoU<sub>2</sub> (blue diamonds) and NiU<sub>2</sub> (red circles) clusters upon modification to account for the loss of spin of the U<sup>IV</sup> centers at low temperatures. Calculated fits to the data are shown as black lines ( $J_{\text{max}}(\text{Co}) = 48 \text{ cm}^{-1}$ ,  $J_{\text{max}}(\text{Ni}) = 19 \text{ cm}^{-1}$ ); see text for details.

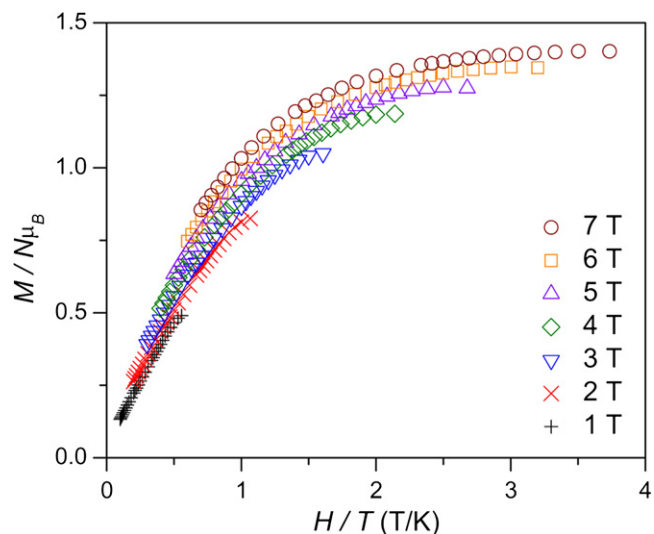


**Fig. 5.** A plot of reduced magnetization,  $M/N\mu_B$  (where  $N$  is Avagadro's number and  $\mu_B$  is the Bohr magneton) versus  $H/T$  for (cyclam)Co[( $\mu$ -Cl)U(Me<sub>2</sub>Pz)<sub>4</sub>]<sub>2</sub>. Data were measured from 1.8 to 10 K at the seven field strengths specified.

in  $\chi_M T$  as temperature is decreased in the ZnU<sub>2</sub> and CoU<sub>2</sub> data sets can be modeled by combining the effects of spin-orbit coupling and ligand field perturbations into a single empirical factor based on the magnetic susceptibility of the ZnU<sub>2</sub> cluster. In ZnU<sub>2</sub>, the deviation of  $\chi_M T$  from the spin-only value of 2.00 emu K/mol is quantified as  $\chi_M T = (2.00 \text{ emu K/mol})/r$ , where  $r$  is a temperature-dependent empirical parameter that accounts for the spin reduction at the individual U<sup>IV</sup> centers for the ZnU<sub>2</sub> complex. For example, at 5 K,  $\chi_M T$  is 0.104 emu K/mol, giving a reduction factor,  $r$  of 19.183 at this temperature. Since the coordination environment of the U<sup>IV</sup> centers is the same for the ZnU<sub>2</sub> and CoU<sub>2</sub> clusters, and  $r$  only describes spin reduction at U<sup>IV</sup>, we assume that  $r$  as a function of temperature is identical for both compounds. Therefore, we can account for the loss of spin on the individual U<sup>IV</sup> centers by multiplying the measured  $\chi_M T$  data for the CoU<sub>2</sub> cluster by the function  $r(T)$  determined for the ZnU<sub>2</sub> cluster. In effect, we have

corrected the CoU<sub>2</sub> data for any spin loss at the individual U<sup>IV</sup> centers, and any deviation from its room temperature  $\chi_{MT}$  value of 4.375 cm<sup>-1</sup> is attributed to exchange coupling between U<sup>IV</sup> and Co<sup>II</sup>. Fitting this spin-corrected CoU<sub>2</sub> data using the Hamiltonian described above gives  $J = 48$  cm<sup>-1</sup>,  $g = 1.80$ , and  $TIP = 1.67 \times 10^{-4}$  emu/mol (Fig. 4, blue diamonds). This treatment was also applied to the NiU<sub>2</sub> data from our previous study to give  $J = 19$  cm<sup>-1</sup>,  $g = 1.85$ , and  $TIP = 5.15 \times 10^{-4}$  emu/mol (Fig. 4, red circles).

As in our previous study of NiU<sub>2</sub>, variable-field magnetization experiments on the CoU<sub>2</sub> cluster show a significant separation of the isofield lines at low temperatures, consistent with a large axial anisotropy (see Fig. 5); however, quantitative methods for fitting these data have yet to produce a reasonable fit. Despite the presence of zero-field splitting, AC magnetic susceptibility measurements performed between 1.8 K and 10 K with oscillating frequencies of up to 1500 Hz did not display any out-of-phase signal indicative of single-molecule magnet behavior.

#### 4. Conclusions

The foregoing results demonstrate the synthesis of a new trinuclear cluster complex, (cyclam)Co[( $\mu$ -Cl)U(Me<sub>2</sub>Pz)<sub>4</sub>]<sub>2</sub>, exhibiting ferromagnetic exchange coupling. As previously noted for the analogous NiU<sub>2</sub> cluster [6g], this ferromagnetic exchange is consistent with a superexchange mechanism in which the spin of the 3d<sub>z<sup>2</sup></sub> orbital of the Co<sup>II</sup> center feeds into the sigma orbital system of the bridging chloride ligands, but is then orthogonal to the 5f<sub>xyz</sub> and 5f<sub>z(x<sup>2</sup>-y<sup>2</sup>)</sub> spin orbitals of the U<sup>IV</sup> centers. Two methods for fitting the temperature-dependence of the magnetic susceptibility data for the cluster – one that treats the uranium and transition-metal contributions separately, and the other that factors spin-orbit coupling, ligand field effects, and exchange coupling into a single empirical factor – enabled estimation of upper and lower bounds for the exchange energy, suggesting 15 cm<sup>-1</sup> <  $J$  < 48 cm<sup>-1</sup>. Importantly, this represents significantly stronger magnetic exchange coupling than typically encountered for lanthanide-containing cluster systems [4]. Thus, the idea that relatively strong magnetic exchange coupling might be realizable by taking advantage of the enhanced radial extension of 5f orbitals of actinide elements appears to be valid. This bodes well for future work attempting to utilize actinide elements in the generation of new single-molecule magnets.

#### Acknowledgements

This research was funded by NSF Grant No. CHE-0617063. We thank the UC President's Postdoctoral Fellowship Program for support of B.M.B. and Drs. Frederick J. Hollander and Allen G. Oliver for expert advice on crystal structure determinations.

#### Appendix A. Supplementary material

CCDC 674709 contains the supplementary crystallographic data for this paper. These data can be obtained free of charge from The Cambridge Crystallographic Data Centre via [www.ccdc.cam.ac.uk/data\\_request/cif](http://www.ccdc.cam.ac.uk/data_request/cif). Supplementary data associated with this article can be found, in the online version, at doi:10.1016/j.ica.2008.03.006.

#### References

- [1] (a) D. Gatteschi, R. Sessoli, *Angew. Chem., Int. Ed.* 42 (2003) 246; (b) D. Gatteschi, R. Sessoli, J. Villain, *Molecular Nanomagnets*, Oxford University Press, Oxford, 2006.
- [2] E. Ruiz, J. Cirera, J. Cano, S. Alvarez, C. Loose, J. Kortus, *Chem. Commun.* (2008) 52.
- [3] (a) N. Ishikawa, M. Sugita, T. Ishikawa, S.-y. Koshihara, Y. Kaizu, *J. Am. Chem. Soc.* 125 (2003) 8694; (b) S. Osa, T. Kido, N. Matsumoto, N. Re, A. Pochaba, J. Mrozinski, *J. Am. Chem. Soc.* 126 (2004) 420; (c) A. Mishra, W. Wernsdorfer, K.A. Abboud, G. Christou, *J. Am. Chem. Soc.* 126 (2004) 15648; (d) C.M. Zaleski, E.C. Depperman, J.W. Kampf, M.L. Kirk, V.L. Pecoraro, *Angew. Chem., Int. Ed.* 43 (2004) 3912; (e) A. Mishra, W. Wernsdorfer, S. Parsons, G. Christou, E.K. Brechin, *Chem. Commun.* (2005) 2086; (f) F. Mori, T. Nyui, T. Ishida, T. Nogami, K.-y. Choi, H. Nojiri, *J. Am. Chem. Soc.* 128 (2006) 1440; (g) J. Tang, I. Hewitt, N.T. Madhu, G. Chastanet, W. Wernsdorfer, C.E. Anson, C. Benelli, R. Sessoli, A.K. Powell, *Angew. Chem., Int. Ed.* 45 (2006) 1729; (h) M. Ferbinteanu, T. Kajiwar, K.-y. Choi, H. Nojiri, A. Nakamoto, N. Kojima, F. Cimpoesu, Y. Fujimura, S. Takaishi, M. Yamashita, *J. Am. Chem. Soc.* 128 (2006) 9008.
- [4] (a) J.-P. Costes, F. Dahan, A. Dupuis, J.-P. Laurent, *Chem. Eur. J.* 4 (1998) 1616; (b) M.L. Kahn, C. Mathoniere, O. Kahn, *Inorg. Chem.* 38 (1999) 3692; (c) C. Benelli, D. Gatteschi, *Chem. Rev.* 102 (2002) 2369. and references cited therein.
- [5] (a) H.M. Crosswhite, H. Crosswhite, W.T. Carnall, A.P. Paszek, *J. Chem. Phys.* 72 (1980) 5103; (b) A.J. Gaunt, S.D. Reilly, A.E. Enriquez, B.L. Scott, J.A. Ibers, P. Sekar, K.I.M. Ingram, N. Kaltsoyannis, M.P. Neu, *Inorg. Chem.* 47 (2008) 29.
- [6] (a) R.K. Rosen, R.A. Andersen, N.M. Edelstein, *J. Am. Chem. Soc.* 112 (1990) 4588; (b) T. Le Borgne, E. Riviere, J. Marrot, P. Thuéry, J.-J. Girerd, M. Ephritikhine, *Chem. Eur. J.* 8 (2002) 774; (c) L. Salmon, P. Thuéry, E. Riviere, J.-J. Girerd, M. Ephritikhine, *Chem. Commun.* (2003) 762; (d) L. Salmon, P. Thuéry, E. Riviere, J.-J. Girerd, M. Ephritikhine, *Dalton Trans.* (2003) 2872; (e) L. Salmon, P. Thuéry, E. Riviere, M. Ephritikhine, *Inorg. Chem.* 45 (2006) 83; (f) E.J. Schelter, J.M. Veauthier, J.D. Thompson, B.L. Scott, K.D. John, D.E. Morris, J.L. Kiplinger, *J. Am. Chem. Soc.* 128 (2006) 2198; (g) S.A. Kozimor, B.M. Bartlett, J.D. Rinehart, J.R. Long, *J. Am. Chem. Soc.* 129 (2007) 10672; (h) E.J. Schelter, D.E. Morris, B.L. Scott, J.D. Thompson, J.L. Kiplinger, *Inorg. Chem.* 46 (2007) 5528; (i) M.J. Monreal, C.T. Carver, P.L. Diaconescu, *Inorg. Chem.* 46 (2007) 7226; (j) P. Christopher, F. Larch, G.N. Cloke, P.B. Hitchcock, *Chem. Commun.* (2008) 82.
- [7] SMART Software Users Guide, Version 5.1, Bruker Analytical X-ray Systems, Inc., Madison, WI, 1999.
- [8] SAINT Software Users Guide, Version 7.0, Bruker Analytical X-ray Systems, Inc., Madison, WI, 1999.
- [9] G.M. Sheldrick, SADABS, Version 2.03, Bruker Analytical X-ray Systems, Inc., Madison, WI, 2000.
- [10] G.M. Sheldrick, SHELXTL, Version 6.12, Bruker Analytical X-ray Systems, Inc., Madison, WI, 1999.
- [11] International Tables for X-ray Crystallography, vol. C, Kluwer Academic Publishers, Dordrecht, 1992.
- [12] (a) I. Bkouche-Waksman, P. L'Haridon, *Acta. Crystallogr. B* 33 (1977) 11; (b) C.S. Campos-Fernandez, B.W. Smucker, R. Clerac, K.R. Dunbar, *Isr. J. Chem.* 41 (2001) 207; (c) O. Schneider, E. Gerstner, F. Weller, K. Dehnicke, *Z. Anorg. Allg. Chem.* 625 (1999) 1101; (d) L.R. MacGillivray, J.L. Atwood, *J. Chem. Crystallogr.* 27 (1997) 453; (e) P.B. Hitchcock, T.H. Lee, G.J. Leigh, *Inorg. Chim. Acta* 348 (2003) 199.
- [13] D.J. Szalda, E. Fujita, C. Creutz, *Inorg. Chem.* 28 (1989) 1446.
- [14] (a) E.K. Brechin, O. Cadore, A. Caneschi, C. Cadiou, S.G. Harris, S. Parsons, M. Voonci, R.E.P. Winpenny, *Chem. Commun.* (2002) 1860; (b) Z.-G. Gu, Q.-F. Yang, W. Liu, Y. Song, Y.-Z. Li, J.-L. Zuo, X.-Z. You, *Inorg. Chem.* 45 (2006) 8895.
- [15] E.A. Schmitt, Ph.D. Thesis, University of Illinois at Urbana-Champaign, 1995.